07,13

Study of the influence of uncontrolled impurities on the structural phase transition in $GdFe_3(BO_3)_4$ using raman scattering

© I.A. Gudim, V.R. Titova, E.M. Moshkina, M.S. Pavlovsky, A.S. Krylov, E.V. Eremin

Kirensky Institute of Physics, Federal Research Center KSC SB, Russian Academy of Sciences, Krasnoyarsk, Russia

E-mail: eev@iph.krasn.ru

Received October 1, 2024
Revised October 8, 2024
Accepted October 9, 2024

When obtaining single-crystal samples using the solution-melt method, the solvent can affect the composition of the grown crystals through the inclusion of uncontrolled impurities, which can significantly affect the properties of the compound. To study the effect of impurities on the structural phase transition in trigonal borate $GdFe_3(BO_3)_4$, the temperature evolution of the Raman spectra of three single-crystal samples of this compound grown from three different solvents based on $Bi_2Mo_3O_{12}$, K_2MoO_4 and Li_2WO_4 was investigated. It was shown that the structural transition temperature T_S of Bi-substituted $GdFe_3(BO_3)_4$ ($T_S = 145$ K) decreased relative to the impurity-free sample ($T_S = 166$ K). The inclusion of impurities from the solvent based on K_2MoO_4 does not affect the T_S temperature, but affects the nature of the phase transition. The analysis of the obtained results was performed jointly with the calculation of the lattice dynamics.

Keywords: rare earth ferroborates, structural phase transitions, Raman scattering, solution-melt method.

DOI: 10.61011/PSS.2024.11.60102.250

1. Introduction

The properties of rare-earth borates with the huntite structure $RM_3(BO_3)_4$ (M = Fe, Cr, Al, Ga, Sc; R = Y, La-Lu) have been intensively studied in recent years. The interest in huntites is associated with a wide range of characteristics, including the magnetoelectric effect, magnetic ordering, spin reorientation, and high optical activity [1–13].

Initially, a method for growing from solution-melts based on potassium trimolybdate $K_2Mo_3O_{10}-B_2O_3$ was developed for isostructured nonlinear optical crystals of trigonal ferroborates $RAl_3(BO_3)_4$ [14]. Later, new solution-melts based on bismuth trimolybdate $Bi_2Mo_3O_{12}-B_2O_3$ were proposed for growing $RAl_3(BO_3)_4$ and $RFe_3(BO_3)_4$ single crystals [15]. Bi_2O_3 and MoO_3 are more strongly bonded in these solution-melts than K_2O_3 and MoO_3. Therefore, the substitution of bismuth and molybdenum in the grown crystal for the rare-earth element was assumed to be relatively weak [16]. However, as it was shown in Ref. [17] by chemical analysis and structural studies for $GdFe_3(BO_3)_4$ ferroborate, Bi^{3+} ions replace the rare-earth ion in an amount up to 5% at., which is nevertheless smaller as compared to the including of potassium and molybdenum [16]. Later this fact was confirmed using magnetic studies [18,19]. In connection with the above, solution-melts based on lithium tungstate Li_2WO_4 have been proposed [18]. It was assumed that ions from the solvent do not enter the crystal matrix in the latter case.

The high-temperature phase of crystals with the huntite structure is characterized by trigonal symmetry (sp. gr. $R32$). A structural phase transition into a phase with spatial symmetry can occur in huntites $P3_121$ depending on the ratio of the radii of rare earth and metallic ions R_{RE}/R_{Me} [4].

The presence of impurities in the crystal matrix changes the effective ion radius and, consequently, R_{RE}/R_{Me} ratio. The temperature of the structural transition T_S should also change in this case, and possibly the nature of the transition itself.

This paper studies of the effect of uncontrolled impurities on the parameters of the structural transition by the study of Raman scattering spectra in ferroborate $GdFe_3(BO_3)_4$ grown from three different solution-melts: based on potassium trimolybdate $K_2Mo_3O_{10}-B_2O_3$, bismuth trimolybdate $Bi_2Mo_3O_{12}-B_2O_3$ and lithium tungstate $Li_2WO_4-B_2O_3$. The magnetic properties of these samples were studied earlier [18,19]. It was shown that ferroborate $GdFe_3(BO_3)_4\{Li_2WO_4\}$ grown from a tungsten-lithium solution-melt does not contain uncontrolled impurities, and, therefore, is the purest compound. The presence of uncontrolled impurities of Bi^{3+} in small amounts, $\sim 5\%$ at. was confirmed for feroborate $GdFe_3(BO_3)_4$ $\{Bi_2Mo_3O_{12}\}$. The situation looks the most complicated for $GdFe_3(BO_3)_4$ $\{K_2Mo_3O_{10}\}$. It has been suggested that both Mo ions (with a valence greater than 3+) and potassium ions K^+ are present as an uncontrolled impurity [19]. At the same time, it is not possible to determine the quantitative and qualitative composition of the impurity due to the large variability of possible combinations.

RSS of ferroborate $GdFe_3(BO_3)_4$ grown from $Bi_2Mo_3O_{12}-B_2O_3$ solution-melt were studied earlier [20]. The temperature variation of the spectrum is analyzed, and the main features associated with the structural phase

transition ($T_S \approx 156$ K) and the low-temperature magnetic phase transition ($T_N \approx 38$ K) are identified. A number of new lines were observed during the structural phase transition $R32 \rightarrow P3_121$. The abrupt change of the position of the centers of many lines of the RS spectrum is characteristic of phase transitions of the first kind. The occurrence of a pronounced „soft" mode in the low-frequency part of the RSS is one of the most important features of this structural phase transition in $GdFe_3(BO_3)_4$, like in other ferroborates characterized by this symmetry change, which indicates that the observed transition belongs to phase transitions close to the tricritical point. The authors of Ref. [20] characterized the structural phase transition at $T_S \approx 156$ K in $GdFe_3(BO_3)_4$ as a „weak first-order phase transition" due to the presence of all these features.

2. Preparation of samples and measurement procedure

Crystals of gadolinium ferroborate $GdFe_3(BO_3)_4$ were grown from three solution-melt systems: based on potassium trimolybdate $K_2Mo_3O_{10}-B_2O_3$, described in detail in Ref. [14], based on bismuth trimolybdate $Bi_2Mo_3O_{12}-B_2O_3$ [15] and based on lithium tungstate $Li_2WO_4-B_2O_3$ [18].

RSS of three nonoriented single crystal samples of huntite $GdFe_3(BO_3)_4$ $\{Bi_2Mo_3O_{12}\}$, $GdFe_3(BO_3)_4$ $\{K_2Mo_3O_{10}\}$ and $GdFe_3(BO_3)_4$ $\{Li_2WO_4\}$ were obtained in the temperature range of 8.5–200 K, in the spectral range of 12–640 cm^{-1} in backscattering geometry using Horiba Jobin Yvon T64000 spectrometer (Horiba, France) with a triple monochromator in the dispersion subtraction mode. The spectral resolution was 2 cm^{-1} (this resolution was achieved using gratings with 1800 hat./mm and 100 μm slits) with a point density of 3 pixel/cm^{-1}. The spectrum was excited by radiation from Spectra-Physics Excelsior solid-state single-mode laser-532-300- CDRH (USA) with a wavelength of 532 nm and a power of < 5 mW on the sample. The low-temperature experiments were conducted using ARSCS204-X1.SS closed-cycle helium cryostat with LakeShore 340 temperature controller. The temperature was controlled by silicon diode LakeShore DT-670SD1.4L. Nonoriented single-crystal samples were studied. RSS of two samples of $GdFe_3(BO_3)_4$ $\{K_2Mo_3O_{10}\}$ and $GdFe_3(BO_3)_4$ $\{Li_2WO_4\}$, as expected, are mixed, containing lines with different polarization [20]. RSS of the sample of $GdFe_3(BO_3)_4$ $\{Bi_2Mo_3O_{12}\}$ corresponds to the polarization (zz), which distinguishes it from the other two samples.

Theoretical calculations were performed within the framework of density functional theory using Perdew-Burke-Ernzerhof exchange-correlation functionals with generalized gradient approximation (PBE-GGA) implemented in the VASP package [21,22]. The number of plane waves was limited by the energy of 600 eV. The Monkhorst-Pack grid [15] was chosen to be equal to $7 \times 7 \times 7$. GGA + U method in the Dudarev approximation [23] was used in the calculation for iron with $U = 4$ eV. $2 \times 2 \times 2$ supercell was constructed to calculate the oscillation frequencies and the force constants were calculated using the small displacement method implemented in PHONOPY [24].

3. Results and discussion

RSS of three single crystal samples of $GdFe_3(BO_3)_4$ obtained from different solvents above ($T = 200$ K) and below ($T = 8.5$ K) the temperature range of the structural phase transition are shown in Figures 1 and 2. The positions of the line centers of the obtained spectra of the three samples do not differ from each other in the high-temperature phase, at $T = 200$ K, upon detailed comparison. When comparing the RSS at different temperatures, it is clearly seen that their appearance changes (Figure 2), new lines appear as a result of the structural phase transition, and the position of the centers of many lines shifts. These changes are typical for all three samples. However, more significant changes are observed in the low-temperature phase, at $T = 8.5$ K, not only relative to the high-temperature phase, but also among samples obtained from different solvents. A new line appears in the low-frequency region of the RS spectra of all samples as a result of the structural phase transition, the frequency of which changes significantly with temperature changes — „soft" mode (insert in Figure 2). The position of the center of this mode is almost identical for the samples obtained from $K_2Mo_3O_{10}$ ($\nu = 57.1$ cm^{-1} at $T = 8.5$ K) and Li_2WO_4 ($\nu = 58.7$ cm^{-1} at $T = 8.5$ K) solution-melts, but significantly differs for sample obtained from $Bi_2Mo_3O_{12}$ solution-melt ($\nu = 52.6$ cm^{-1} at $T = 8.5$ K).

The temperature evolution of the RS lines of the studied samples was analyzed in the temperature range of $T = 8.5$–200 K for a more detailed study of the causes of the discrepancy obtained and for studying the nature of the structural phase transition. Figure 3 shows the temperature dependence of the position of the center of the line in the spectral range of 470–480 cm^{-1}.

Similar changes are observed in the temperature dependence for a sample obtained from a solvent based on K_2MoO_4 — however, the slope of the curve is much smaller, and the position of the center of the line changes over a wider temperature range, smearing the transition region. The structural phase transition in a sample obtained from a solvent based on $Bi_2Mo_3O_{12}$ occurs only at $T_S = 145$ K, which is by $\Delta T = 21$ K lower than in the presumably „pure" $GdFe_3(BO_3)_4$. The slope of the temperature curve in the transition region corresponds to the sample obtained from Li_2WO_4 solvent.

Thus, a significant difference of phase transition temperatures was found due to the introduction of uncontrolled impurities into $GdFe_3(BO_3)_4-Bi^{3+}$ from a solvent based on $Bi_2Mo_3O_{12}$. The difference of transition temperatures of samples obtained by different methods was already noted earlier [25] in the study of this structural phase

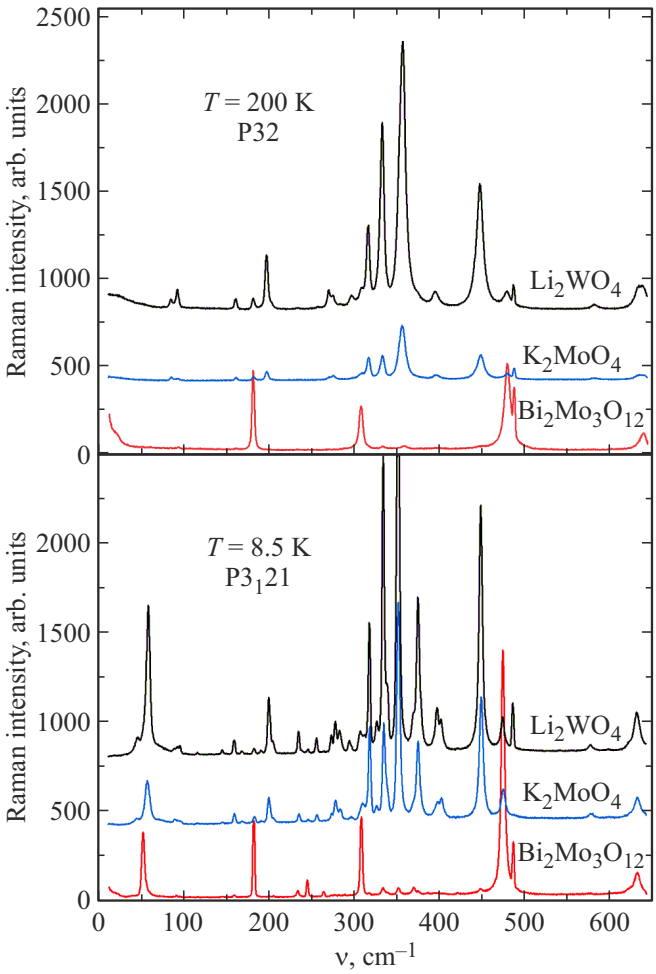

Figure 1. RS of $GdFe_3(BO_3)_4$ crystals obtained from solvents based on $Bi_2Mo_3O_{12}$ (red), K_2MoO_4 (blue) and Li_2WO_4 (black), measured at $T = 200$ K (top) and $T = 8.5$ K (at the bottom).

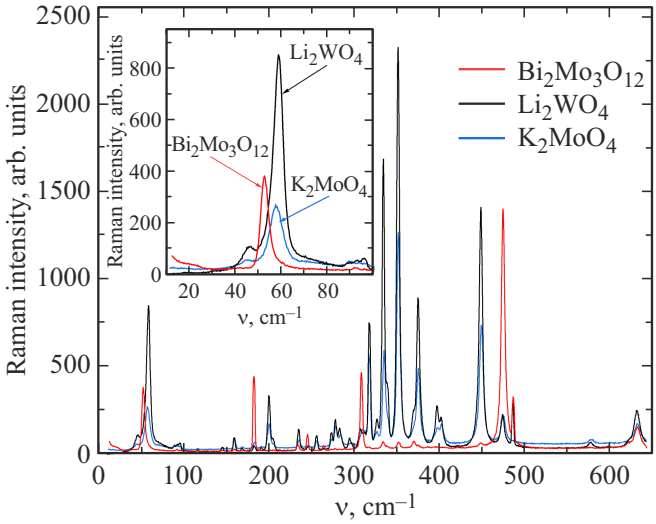

Figure 2. Comparison of RS spectra of $GdFe_3(BO_3)_4$ crystals obtained from solvents based on $Bi_2Mo_3O_{12}$ (red), K_2MoO_4 (blue) and Li_2WO_4 (black) in the low-temperature phase. The insert shows a comparison of the low-frequency part of the spectra, including the „soft“ mode.

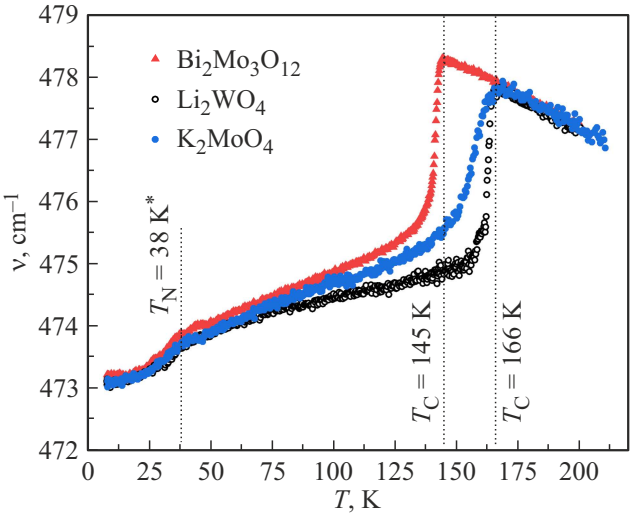

Figure 3. Temperature dependence of the position of the center of the line of the spectral range of 470–480 cm^{-1} of $GdFe_3(BO_3)_4$ crystals obtained from solvents based on $Bi_2Mo_3O_{12}$ (red), K_2MoO_4 (blue) and Li_2WO_4 (black). $T_N = 38$ K data are obtained from Ref. [20].

transition in $GdFe_3(BO_3)_4$. The temperature of this phase transition was equal to $T_S \approx 155-156$ K in the single crystal sample studied in Ref. [20], which was also obtained from a solution-melt based on $Bi_2Mo_3O_{12}$, which is 10 K higher than the similar value obtained for $GdFe_3(BO_3)_4$, grown from the same solvent and studied in this paper. The temperature of the structural phase transition of a polycrystalline sample containing no impurities was equal to $T_S \approx 176$ K according to the data in Ref. [26]. It can be seen from the presented data that the structural phase transition in $GdFe_3(BO_3)_4$ demonstrates significant sensitivity to bismuth impurity.

The introduction of potassium and molybdenum cations into $GdFe_3(BO_3)_4$ crystal from a solvent based on K_2MoO_4 changes the nature of the phase transition, expanding the transition region, changes of the position of the center of the line become smooth and more characteristic of the second-order phase transition, the transformation in the lattice occurs over a wider temperature range. It can be seen upon detailed examination that all three curves again reach the same value only in the region of the low-temperature magnetic transition, which occurs at $T_N = 38$ K (Figure 3), according to the literature data [20].

Figure 4 shows the temperature dependences of the line width of the spectral range of 470–480 cm^{-1} of the studied samples. All three dependences exhibit a sharp jump at the temperature of the structural phase transition corresponding to the broadening of the line in case of the phase transition. Since the width of the line in the RSS can indicate the degree of disordering of the bonds involved in this oscillation, it is possible to state that this dependence demonstrates an increase of the proportion of „disorder“ in case of the phase transition [27].

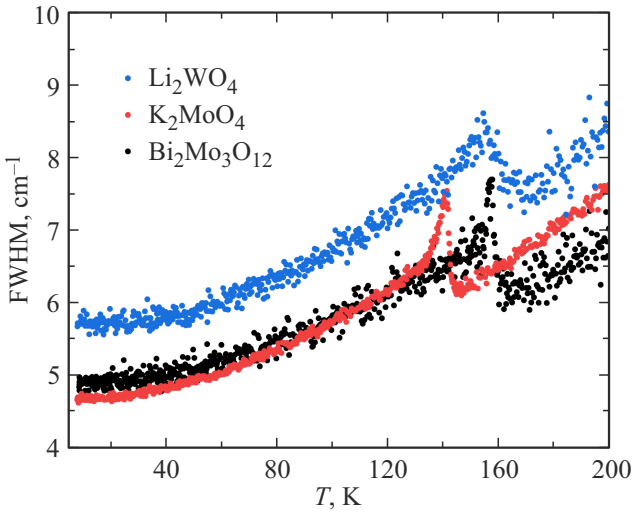

Figure 4. Temperature dependence of the line width of the spectral range of 470–480 cm^{-1} of $GdFe_3(BO_3)_4$ crystals obtained from solvents based on $Bi_2Mo_3O_{12}$ (red), K_2MoO_4 (blue) and Li_2WO_4 (black). $T_N = 38$ K data are obtained from Ref. [20].

It can be concluded by comparing the curves with each other that the this peak width of dependence for a crystal obtained from a solvent based on K_2MoO_4 is greater than for the other two samples. The line width for this crystal is also greater than the corresponding values for other samples up to $T = 8.5$ K, which may indicate a large proportion of „disorder“ in this sample caused by the introduction of impurities of potassium and molybdenum.

Temperature dependence of the position of the center of the „soft“ mode in $GdFe_3(BO_3)_4$ obtained from solvents based on $Bi_2Mo_3O_{12}$ and comparison of the temperature course of this mode of all three samples is shown in Figure 5. The appearance and motion of the „soft“ mode is very abrupt in the transition area as can be seen from the figure: the position of the center of the corresponding line changes to $\Delta\nu \approx 23$ cm^{-1} for $\Delta T = 2$ K. Further, a more monotonous frequency change is observed. When comparing the curves for all three samples, the slope of the curves is similar in the low-temperature region. At temperatures $T < T_N$, the dependences of the positions of the centers of the Raman lines (Figures 3, 5) also show features associated with the magnetic phase transition.

Model calculations of lattice dynamics and phonon spectra were performed based on first principles for a qualitative explanation of the observed results. The primitive ferroborate cell has the shape of a rhombohedron with an angle between the lattice vectors $\alpha > 90°$. The shape of the Brillouin zone and its boundary points for this case are shown in Figure 6. The axis of symmetry of the third order passes through the points Γ and Q, the axis of symmetry of the second order passes through the points Γ and F. The points Λ and Λ_1 are translated into each other by the axis of symmetry of the second order. The phase transition $R32\,(Z = 1) \rightarrow P3_121\,(Z = 3)$ is associated with one component of the two-dimensional complete representation Λ_3 according to the results of the group-theoretic analysis (see, for example, the ISOTROPY program [24]) (representation star Λ_3 contains two vectors $\mathbf{q}_\Lambda = 1/3(-2\mathbf{b}_1 + \mathbf{b}_2 + \mathbf{b}_3)$ and $\mathbf{q}_{\Lambda 1} = -1/3(-2\mathbf{b}_1 + \mathbf{b}_2 + \mathbf{b}_3)$).

The equilibrium values of the lattice parameters and atomic coordinates were calculated for $GdFe_3(BO_3)_4$ and $BiFe_3(BO_3)_4$) compounds which were later used to calculate the lattice dynamics. The lattice parameters of gadolinium ferroborate ($a = 9.6332$ Å, $c = 7.6449$ Å, hexagonal arrangement) are in good agreement with experimental data [17] ($a = 9.5203$ Å, $c = 7.5439$ Å), the difference is no more than 1.5%. There are no structural data in the open database for bismuth ferroborate, the calculated lattice parameters were $a = 9.6863$ Å, $c = 7.6787$ Å.

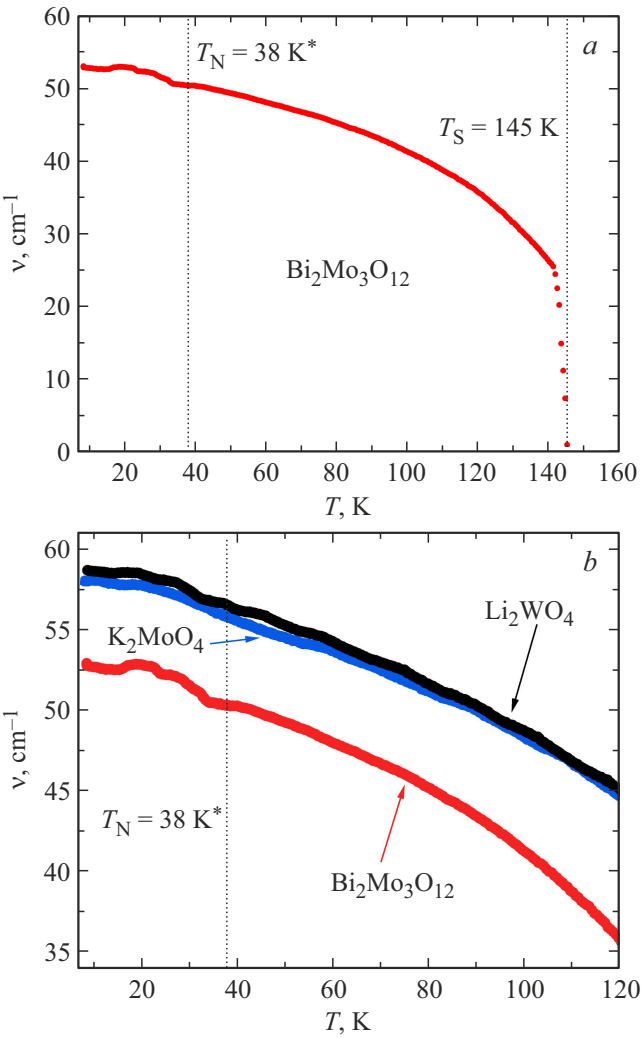

Figure 5. Temperature behavior of the center position of the „soft“ mode in $GdFe_3(BO_3)_4$ obtained from solvents based on $Bi_2Mo_3O_{12}$ (*a*); comparison of the temperature course of the position of the centers of soft modes of $GdFe_3(BO_3)_4$ crystals obtained from solvents based on $Bi_2Mo_3O_{12}$ (red), K_2MoO_4 (blue) and Li_2WO_4 (black) (*b*). $T_N = 38$ K data are obtained from Ref. [20].

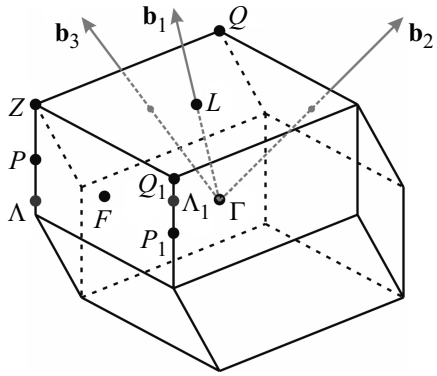

Figure 6. The Brillouin zone with points of symmetry and vectors of the inverse lattice of the trigonal symmetry group $R32$.

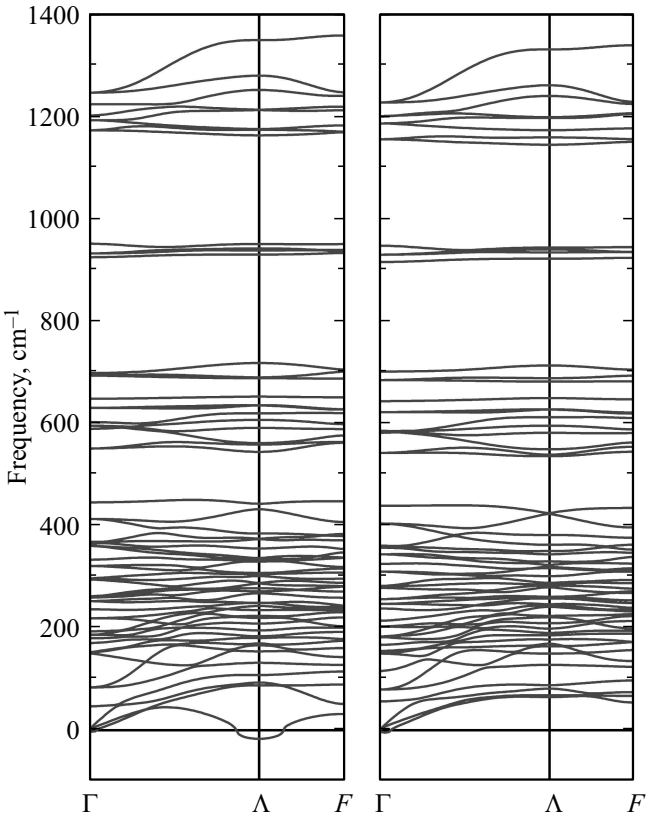

Figure 7. Theoretically calculated phonon spectra of crystals $GdFe_3(BO_3)_4$(left) and $BiFe_3(BO_3)_4$(right) for the direction $\Gamma \to \Lambda \to F$.

Complete phonon spectra in the phase $R32$ for the studied crystals were plotted based on the calculation of the dynamics of the crystal lattice. No significant differences were found in the phonon spectra of the studied compounds (except the vicinity of the point Λ_1), neither in the frequencies of the phonon modes, nor in the nature of their dispersion. The maximum differences in the oscillation frequencies of these crystals in the high-frequency region of the spectrum do not exceed $20\,cm^{-1}$, the differences do not exceed $10\,cm^{-1}$ in the rest of the spectrum. Figure 7, *a* and *b* show the phonon spectra of $GdFe_3(BO_3)_4$ and $BiFe_3(BO_3)_4$ crystals for the direction $\Gamma \to \Lambda \to F$.

The main feature of the obtained phonon spectra is the presence of deflection of the acoustic oscillation branch in the vicinity of the point Λ (and Λ_1) in $GdFe_3(BO_3)_4$ compound and its complete absence in $BiFe_3(BO_3)_4$ compound.

The deflection of one of the transverse acoustic branches with a minimum at the point Λ is clearly visible in Figure 7, *a*, while the frequency of the mode at the point Λ has an imaginary value (a soft mode occurs). The presence of an imaginary mode in such calculations indicates the instability of the crystal lattice with respect to the distortion of the structure along its corresponding eigenvector. Indeed, the shift of ions along the eigen vector of the soft mode at the point Λ with the corresponding cell tripling is energetically favorable for $GdFe_3(BO_3)_4$ compound and leads to a structure with the symmetry group $P3_121$.

A complete absence of unstable (imaginary) modes of fluctuations or anomalous softening of any modes throughout the Brillouin zone was determined in the calculated phonon spectra for $BiFe_3(BO_3)_4$) crystal. This indicates the complete stability of the phase $R32$ of this compound in relation to any types of structural instability, i.e., no phase transitions of the displacement type can occur in this crystal within the framework of the approachused.

It is possible to conclude based on the obtained calculated data that the substitution of gadolinium ions with bismuth ions in $GdFe_3(BO_3)_4$ will stabilize the crystal lattice of the compound, which in turn will lead to a decrease of the temperature of the structural phase transition $R32 \to P3_121$. Apparently, a similar phenomenon can be observed in all rare-earth oxyborates with a huntite structure undergoing a phase transition $R32 \to P3_121$.

Unfortunately, it is not possible to perform similar calculations for the case of oxyborates with the huntite structure, which would contain molybdenum and potassium ions because of the lack of information on which positions and in which valence state these ions can enter the structure.

4. Conclusion

The raman scattering spectra (RSS) of ferroborate $GdFe_3(BO_3)_4$ grown from three different solution-melts were studied in this paper: based on potassium trimolybdate $K_2Mo_3O_{10}-B_2O_3$, bismuth trimolybdate $Bi_2Mo_3O_{12}-B_2O_3$ and lithium tungstate $Li_2WO_4-B_2O_3$.

A significant difference of the temperature of the structural phase transition T_S $R32 \to P3_121$ for Bi-substituted $GdFe_3(BO_3)_4$, $(K_2Mo_3O_{10}-B_2O_3)$ relative to the undoped sample ($T_S = 166\,K$). It is shown that the introduction of impurities of K and Mo ions from the solvent based on K_2MoO_4 does not affect the temperature of T_S, but affects the nature of the phase transition.

The nature of the phase transition was elucidated by ab initio calculations in the framework of density functional theory for $GdFe_3(BO_3)_4$ and $BiFe_3(BO_3)_4$ compounds.

The complete phonon spectra of the studied crystals were constructed based on the calculation of the dynamics of the crystal lattice. It was shown that the main feature of the obtained phonon spectra is the presence of deflection of the acoustic branch of vibrations in the vicinity of the point Λ (and Λ_1) in $GdFe_3(BO_3)_4$ compound and its complete absence in $BiFe_3(BO_3)_4$ compound. This means that the substitution of gadolinium ions Gd^{3+} with bismuth ions Bi^{+} in $GdFe_3(BO_3)_4$) will stabilize the crystal lattice of the compound, and this in turn will decrease the temperature of the structural phase transition $R32 \rightarrow P3_121$.

Funding

This study was supported by grant No. 22-12-20019 provided by the Russian Science Foundation and the Krasnoyarsk Regional Science Foundation

Conflict of interest

The authors declare that they have no conflict of interest.

References

[1] A.K. Zvezdin, S.S. Krotov, A.M. Kadomtseva, G.P. Vorobiev, Yu.F. Popov, A.P. Pyatakov, L.N. Bezmaternykh, E.N. Popova. Pis'ma v ZhETF **81**, 335 (2005). (in Russian).
[2] E.A. Popova, D.V. Volkov, A.N. Vasiliev, A.A. Demidov, N.P. Kolmakova, I.A. Gudim, L. N. Bezmaternykh, N. Tristan, Yu. Skourski, B. Büchner, C. Hess, R. Klingeler. Phys. Rev. B **75**, 224413 (2007).
[3] E.A. Popova, N.I. Leonyuk, M.N. Popova, E.P. Chukalina, K.N. Boldyrev, N. Tristan, R. Klingeler, B. Büchner. Phys. Rev. B **76**, 054446 (2007).
[4] A.M. Kadomtseva, Yu.F. Popov, G.P. Vorob'ev, A.P. Pyatakov, S.S. Krotov, K.I. Kamilov, V.Yu. Ivanov, A.A. Mukhin, A.K. Zvezdin, A.M. Kuz'menko, L.N. Bezmaternykh, I.A. Gudim, V.L. Temerov. FNT **36**, 640 (2010). (in Russian).
[5] J.E. Hamann-Borrero, S. Partzsch, S. Valencia, C. Mazzoli, J. Herrero-Martin, R. Feyerherm, E. Dudzik, C. Hess, A. Vasiliev, L. Bezmaternykh, B. Buchner, J. Geck. Phys. Rev. Lett. **109**, 267202 (2012).
[6] A.I. Begunov, A.A. Demidov, I.A. Gudim, E.V. Eremin. Pis'ma v ZhETF **97**, 611 (2013). (in Russian).
[7] N.V. Volkov, I.A. Gudim, E.V. Eremin, A.I. Begunov, A.A. Demidov, K.N. Boldyrev. Pis'ma v ZhETF **99**, 72 (2014). (in Russian).
[8] K.N. Boldyrev, M. Diab, I.A. Gudim, M.N. Popova. ZhETF, **164**, 563 (2023). (in Russian).
[9] A.I. Popov, D.I. Plokhov, A.K. Zvezdin. Phys. Rev. B **87**, 024413 (2013).
[10] R.P. Chaudhury, B. Lorenz, Y.Y. Sun, L.N. Bezmaternykh, V.L. Temerov, C.W. Chu. Phys. Rev. B **81**, 220402 (2010).
[11] K.-C. Liang, R.P. Chaudhury, B. Lorenz, Y.Y. Sun, L.N. Bezmaternykh, V.L. Temerov, C.W. Chu. Phys. Rev. B **83**, 180417(R) (2011).
[12] K.-C. Liang, R.P. Chaudhury, B. Lorenz, Y.Y. Sun, L.N. Bezmaternykh, I.A. Gudim, V.L. Temerov, C.W. Chu. J. of Phys.: Conf. Ser. **400**, 032046 (2012).
[13] N.V. Volkov, I.A. Gudim, A.A. Demidov, E.V. Eremin. Pis'ma v ZhETF **101**, 347 (2015). (in Russian).
[14] N.I. Leonyuk, L.I. Leonyuk. Progress in Crystal Growth and Characterization. **31**, 179 (1995).
[15] L.N. Bezmaternykh, V.L. Temerov, I.A. Gudim, N.A. Stolbovaya. Crystallography Reports **50**, *S1*, 97 (2005).
[16] K.N. Boldyrev, M.N. Popova, M. Bettinelli, V.L. Temerov, I.A. Gudim, L.N. Bezmaternykh, P. Loiseau, G. Aka, N.I. Leonyuk. Optical Materials **34**, *11*, 1885 (2012).
[17] I.S. Lyubutin, A.G. Gavriliuk, N.D. Andryushin, M.S. Pavlovskiy, V.I. Zinenko, M.V. Lyubutina, I.A. Troyan, E.S. Smirnova. Cryst. Growth Des. **19**, *12*, 6935 (2019).
[18] I.A. Gudim, E.V. Eremin, N.V. Mikhashenok, V.R. Titova. FTT **65**, *2*, 243 (2023). (in Russian).
[19] E.V. Eremin, I.A. Gudim, V.R. Titova. FTT **65**, *11*, 1925 (2023). (in Russian).
[20] D. Fausti, A.A. Nugroho, Paul H.M. van Loosdrecht, S.A. Klimin, M.N. Popova, L.N. Bezmaternykh. Phys. Rev. B **74**, 024403 (2006).
[21] G. Kresse, D. Joubert. Phys. Rev. B **59**, 1758 (1999).
[22] G. Kresse, J. Furthmüller. Phys. Rev. B **54**, 11169 (1996).
[23] J.P. Perdew, K. Burke, M. Ernzerhof. Phys. Rev. Lett. **77**, 3865 (1996).
[24] A. Togo, T. Tanaka. Scr. Mater. **108**, 1 (2015).
[25] K.V. Frolov, I.S. Lyubutin, E.S. Smirnova, O.A. Alekseeva, I.A. Verin, V.V. Artemov, S.A. Kharlamova, L.N. Bezmaternykh, I.A. Gudim. J. Alloys and Comp. **671**, 545 (20016).
[26] Yukio Hinatsu, Yoshihiro Doi, Kentaro Ito, Makoto Wakeshima, Abdolali Alemi. J. Solid State Chemistry **172**, 438 (2003).
[27] A.S. Krylov, E.M. Kolesnikova, L.I. Isaenko, S.N. Krylova, A.N. Vtyurin. Cryst. Growth Des. **14**, *3*, 923–927 (2014).

Translated by A.Akhtyamov